Synthetic Metals 161 (2011) 2434–2440

Contents lists available at SciVerse ScienceDirect

Synthetic Metals

journal homepage: www.elsevier.com/locate/synmet

Synthesis and photovoltaic property of donor–acceptor type conjugated polymer containing carbazole and 4,7-dithiazolylbenzothiadiazole moiety utilized as a promising electron withdrawing unit

Jang Yong Lee, Kwan Wook Song, Ho Jun Song, Doo Kyung Moon*

Department of Materials Chemistry and Engineering, Konkuk University, 1 Hwayang-dong, Gwangjin-gu, Seoul 143-701, Republic of Korea

ARTICLE INFO

Article history:
Received 28 March 2011
Received in revised form 8 September 2011
Accepted 11 September 2011
Available online 28 September 2011

Keywords:
Organic photovoltaics
Electron withdrawing material
Conjugated polymers
Copolymerization

ABSTRACT

A donor–acceptor type low band gap conjugated polymer that was composed of carbazole and 4,7-dithiazolylbenzothiadiazole (DTzBT), i.e. Poly [N-9′-heptadecanyl-2,7-carbazole-alt-5,5-(4′,7′-di-2-thiazol-2′,1′,3′-benzothiadiazole)] (PCDTzBT), was synthesized through the Suzuki coupling polymerization for organic photovoltaics. According to the simulated electronic properties, the synthesized polymer exhibited a better balanced energy level than the polymer that included the 4,7-dithienylbenzothiadiazole (DTBT) moiety. In optical and electrochemical experiments, it exhibited a band gap as low as 1.85 eV and well balanced HOMO and LUMO energy levels of −5.54 and −3.65 eV, respectively. A PCE of 0.448% was observed in the device that used the PCDTzBT/PC_{71}BM blend film as the active layer. In spite of the well-balanced energy level and low band gap, it is believed that the low PCE value depended on the low molecular weight.

1. Introduction

Semiconducting polymers have been developed into useful materials for a variety of applications, such as photovoltaic cells (PVs) [1–9], thin-film transistors (TFTs) [10–13], and light-emitting diodes [14–18]. In the past few years, photovoltaic devices based on conjugated polymers have been extensively studied. Particularly, various polymer materials have been vigorously investigated in order to enhance the photovoltaic efficiency and oxidative stability in the most widely used configuration of polymer solar cells, bulk heterojunction type devices [19–23].

A photon absorption property that has a wide solar spectrum and well-balanced energy levels has been regarded as necessary for promising polymer photovoltaic materials [24]. In order to reduce the band gap and optimize the highest occupied molecular orbital (HOMO) and lowest unoccupied molecular orbital (LUMO) energy levels, the donor/acceptor (DA) conjugated system has been regarded as an effective method since the polymer band gap and HOMO/LUMO energy levels are easily controlled by adjusting the molecular orbital overlapping effect, which is induced from the intra-chain charge transfer from the donor to the acceptor [25].

In DA type copolymers, the electronic and chemical properties of the electron-withdrawing moiety are very important factors for determining that of DA type copolymer. A strong electron affinity, structural planarity, and various resonance structures are key factors for promising electron withdrawing units in DA type low band gap polymers [26]. From this perspective, 2,1,3-benzothiadiazole, which is a well-known electron-withdrawing molecule, has been used in various electronic materials [27–30]. In many cases, this unit was linked with thiophenes for further modification since the thiophenes can be easily functionalized. However, introduction of electron-donating thiophene groups decrease the electron withdrawing property of benzothiadiazole. If a heterocyclic ring, which has not only comparable electronic and structural properties to thiophene but also stronger electron affinity than it, is neighbored with benzothiadiazole in the polymer backbone as a spacer, the band gap and energy levels of the copolymer will be controlled efficiently.

Several years ago, the Yamashita group demonstrated the electronic and structural properties of 4,7-dithiazolylbenzothiadiazole (DTzBT) and its potential use as an outstanding material for OTFTs of thiazoles-linked benzothiadiazole [31]. Despite its outstanding properties, there were no further studies regarding materials combined with the DTzBT unit. In this context, we took note of the DTzBT unit as an electron-accepting building block for organic photovoltaic materials. Since thiazole has a stronger electron affinity than thiophenes, it is expected that the intramolecular interaction between the electron-donating unit and electron-withdrawing unit is efficiently induced in the polymer backbone. In addition, the thiazole ring is expected to reduce the steric interactions between

* Corresponding author. Fax: +82 2 450 3498.
E-mail address: dkmoon@konkuk.ac.kr (D.K. Moon).

0379-6779/$ – see front matter © 2011 Elsevier B.V. All rights reserved.
doi:10.1016/j.synthmet.2011.09.021

the neighboring rings, resulting in increases of the planarity of the molecule, which is favorable for intermolecular π–π interactions.

Herein, the synthesis and organic photovoltaic device performance of a new conjugated copolymer based on the DTzBT unit, that is poly[N-9′-heptadecanyl-2,7-carbazole-alt-4,7-dithiazolylbenzothiadiazole] (PCDTzBT), is reported. As an electron-donating materials, carbazole was introduced in polymer backbone since carbazole derivatives exhibited good hole-transporting property as well as good oxidative stability [32,33]. The synthesis, electrochemical behavior, optical properties, and photovoltaic property of the polymer are discussed. Furthermore, a potential of 4,7-dithiazolylbenzothiadiazole unit as a dopant material for OLEDs is discussed.

2. Experimental

2.1. Instruments and characterization

All of the reagents and chemicals were purchased from Aldrich and used as received unless otherwise specified. The ^{1}H NMR (400 MHz) spectra were recorded using a Brüker AMX400 spectrometer in $CDCl_3$, and the chemical shifts were recorded in units of ppm with TMS as the internal standard. The elemental analyses were measured with EA1112 using a CE Instrument. The absorption spectra were recorded using an Agilent 8453 UV-visible spectroscopy system. The solutions that were used for the UV–visible spectroscopy measurements were dissolved in chloroform at a concentration of 10 μg/mL. The films were drop-coated from the chloroform solution onto a quartz substrate. The PL spectra were measured using a Hitachi F-4500 spectrophotometer. The solutions that were used for the UV–visible spectroscopy and photoluminescence (PL) efficiency measurements were dissolved in chloroform at a concentration of 1 mg/mL. The films were drop-coated from the chloroform solution onto a quartz substrate. All of the GPC analyses were carried out using THF as the eluent and a polystyrene standard as the reference. The TGA measurements were performed using a TA Instrument 2050. The cyclic voltammetric waves were produced using a Zahner IM6eX electrochemical workstation with a 0.1 M acetonitrile (substituted with nitrogen in 20 min) solution containing Bu_4NPF_6 as the electrolyte at a constant scan rate of 50 mV/s. ITO, a Pt wire, and silver/silver chloride [Ag in 0.1 M KCl] were used as the working, counter, and reference electrodes, respectively. The electrochemical potential was calibrated against Fc/Fc^+. The current–voltage (I–V) curves of the photovoltaic devices were measured using a computer-controlled Keithley 2400 source measurement unit (SMU) that was equipped with a Peccell solar simulator under an illumination of AM 1.5G (100 mW cm^{-2}).

2.2. Fabrication and characterization of polymer solar cells

All of the bulk-heterojunction PV cells were prepared using the following device fabrication procedure. The glass/ITO substrates [Sanyo, Japan (10 Ω/γ)] were sequentially lithographically patterned, cleaned with detergent, and ultrasonicated in deionized water, acetone, and isopropyl alcohol. Then the substrates were dried on a hotplate at 120 °C for 10 min and treated with oxygen plasma for 10 min in order to improve the contact angle just before the film coating process. Poly(3,4-ethylenedioxythiophene):poly(styrene-sulfonate) (PEDOT:PSS, Baytron P 4083 Bayer AG) was passed through a 0.45 μm filter before being deposited onto ITO at a thickness of ca. 40 nm by spin-coating at 4000 rpm in air and then it was dried at 120 °C for 20 min inside a glove box. A blend of the polymer and PCBM (1:4, w/w) was dissolved in ODCB (the concentration was controlled adequately in the 0.5 wt% range), filtered through a 0.45 μm poly(tetrafluoroethylene) (PTFE) filter, and then spin-coated (1100 rpm, 40 s) on top of the PEDOT:PSS layer. The sample was then heated at 120 °C for 10 min inside a glove box filled with nitrogen. The device fabrication was completed by depositing thin layers of BaF_2 (1 nm), Ba (2 nm), and Al (200 nm) at pressures less than 10^{-6} Torr. The active area of the device was 4.0 mm^2. Finally, the cell was encapsulated using UV-curing glue (Nagase, Japan). The illumination intensity was calibrated using a standard Si photodiode detector that was equipped with a KG-5filter. The output photocurrent was adjusted to match the photocurrent of the Si reference cell in order to obtain a power density of 100 mW cm^{-2}. After the encapsulation, all of the devices were operated under an ambient atmosphere at 25 °C.

2.3. Materials

All reagents and chemicals were purchased from Aldrich. Chloroform was dried over $CaCl_2$ and THF, toluene was dried over sodium under a nitrogen atmosphere. Other reagents and chemicals were used as received. 4,7-Dibromo-2,1,3-benzothiadiazole (1) [34,35], 2,7-bis(4′,4′,5′,5′-tetramethyl-1′,3′,2′-dioxaborolan-2′-yl)-N-9″-heptadecanylcarbazole (5) [36] were prepared as described in the literature.

2.3.1. 2-Tributylstannyl thiazole (2)

To a stirred solution of thiazole (1 g, 11.7 mmol) in diethyl ether (45 mL), n-butyllithium (2.5 M in hexane) (5.14 mL, 12.8 mmol) was added slowly at −50 °C. The mixture was stirred at −50 °C for 1 h and then a solution of tributylstannyl chloride (4.16 g, 12.8 mmol) was added dropwise. After one additional hour, the resulting mixture was warmed to room temperature and stirred overnight. The reaction mixture was washed with saturated aqueous sodium bicarbonate and brine, dried with sodium sulfate, and the solvent was removed under reduced pressure. Brown liquid Yield 2.5 g (86.18%) ^{1}H NMR (400 MHz, $CDCl_3$, δ, ppm): 8.17 (d, 1H), 7.97 (d, 1H), 1.34 (m, 6H), 1.24–1.20 (m, 12H), 0.93–0.87 (m, 9H); ^{13}C NMR (100 MHz, $CDCl_3$, δ, ppm): 173.914, 145.487, 121.242, 29.024, 27.364, 13.779, 11.327.

2.3.2. 4,7-Di(thiazol-2-yl)benzo[c][1,2,5]thiadiazole (3)

To a solution of 4,7-dibromo-2,1,3-benzothiadiazole (1.91 g) and 2-tributylstannyl thiazole (5.34 g) in anhydrous toluene (120 mL), $Pd(PPh_3)_4$ (750 mg) was added. The mixture was heated at 100 °C and then refluxed. After 12 h, the mixture was cooled at room temperature, the solvent was removed under reduced pressure, and the solution was washed with water and dried by sodium sulfate. The residue was purified by column chromatography (eluent chloroform). Recrystallization from chloroform gave the title compound yellow powder (1.18 g, 60.09%). ^{1}H NMR (400 MHz, $CDCl_3$, δ, ppm): 8.76 (s, 2H), 8.07 (d, 2H), 7.64 (d, 2H).

2.3.3. 4,7-Bis(5-bromothiazol-2-yl)benzo[c][1,2,5]thiadiazole (4)

To a solution of 4,7-di(thiazol-2-yl)benzo[c][1,2,5]thiadiazole (1.195 g) in chloroform (50 mL) and DMF (50 mL), NBS (1.547 g) was added and heated at 60 °C. After 24 h, the mixture was cooled at room temperature, extracted with chloroform, washed with water, and dried by sodium sulfate. The solvent was removed from the under reduced pressure and recrytallization in chloroform gave the title compound as a light red solid (1.201 g (66.1%) ^{1}H NMR (400 MHz, $CDCl_3$, δ, ppm): 8.69 (s, 2H), 7.94 (s, 2H).

2.3.4. PCDTzBT

Compound 2 (0.225 g), compound 5 (0.143 g) and tetrakis(triphenylphosphine) palladium(0) ($PPh_3)_4Pd(0)$ (6 mg)

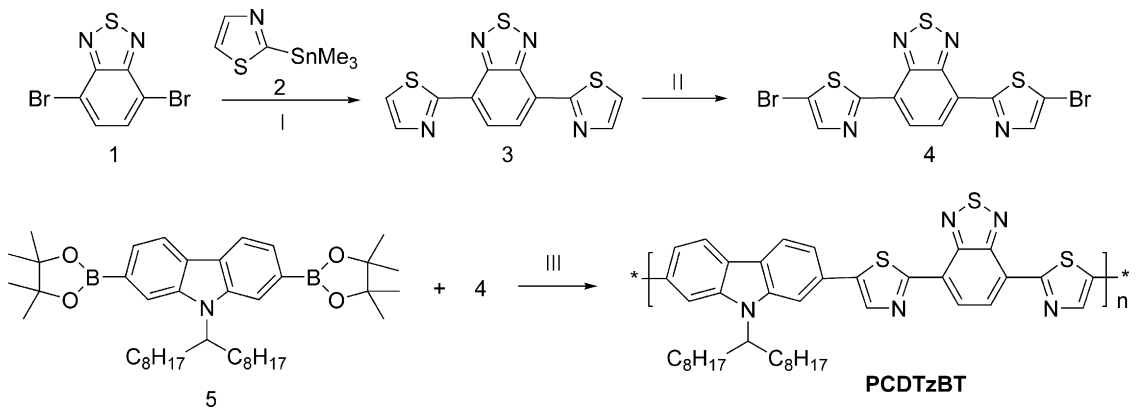

Scheme 1.

were dissolved in a mixture of dry toluene (3 mL) and aqueous 2 M K_2CO_3 (2 mL). The solution was refluxed with vigorous stirring under a nitrogen atmosphere for 2.5 h. The polymerization solution was poured into methanol with stirring, and the resulting precipitate was dissolved in $CHCl_3$ and washed with dilute HCl. The organic layer was separated using a separatory funnel and evaporated. The solid residue was dissolved again in toluene for reprecipitation. The precipitated polymer was filtered off, and dissolved again in $CHCl_3$. The polymer solution was slowly poured into intensively stirred methanol. The precipitated polymer was filtered off and washed with dilute HCl, NH_4OH, and water. The crude polymer was washed for 24 h in a Soxhlet apparatus using methanol, acetone, hexane, and chloroform to remove oligomers and catalyst residues. Dark violet solid (0.2 g (65%) ^{1}H NMR (400 MHz, $CDCl_3$, δ, ppm): 8.81–7.31 (ArH, 10H), 4.66 (–CH, H), 2.4–2.0(–CH_2, 4H), 1.45–0.95 (–CH_2, 24H), 0.78 (–CH_3, 6H).

3. Results and discussion

3.1. Synthesis and characterization

The synthesis process for the monomers and polymers is shown in Scheme 1. The molecular weight of the polymers was measured using GPC, and polystyrene was used as the standard with THF as the eluent. The number average molecular weight (M_n) and the weight average molecular weight (M_w) were 5.5 kg/mol and 7.0 kg/mol, respectively. The thermal properties of PCDTzBT were investigated using thermogravimetric analysis (TGA) at a heating rate of 10 K/min. The polymer exhibited decomposition temperatures (T_d) near 315 °C, which indicated that PCDTzBT exhibited good thermal stability, making it applicable for use in polymer solar cells and other optoelectronic devices. The molecular weight measurements and thermal property results are shown in Table 1.

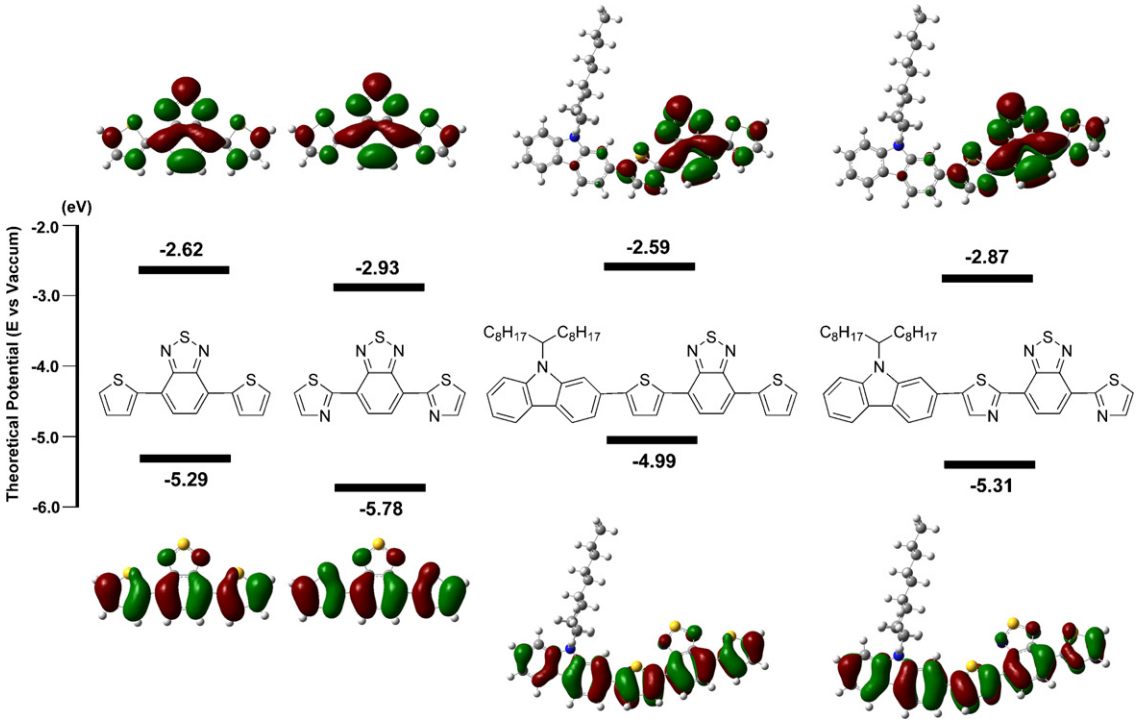

Fig. 1. Theoretical HOMO and LUMO energy levels.

Table 1
Molecular weights and thermal property of PCDTzBT.

Polymer	M_n (kg/mol)	M_w (kg/mol)	M_w/M_n	T_d (°C)
PCDTzBT	5.5	7.0	1.25	315

Molecular weights and ploydispersity indexes determined by GPC in THF on the basis of polystyrene calibration.

3.2. Theoretical calculations

Predicting the behavior of both the HOMO and LUMO energy levels for new polymers is crucial for making a rational design of optimized BHJ solar cells. In the present work, we estimated the HOMO and LUMO energy levels of the repetitive units of the corresponding alternating copolymers by using density functional theory (DFT), as approximated by the B3LYP functional and employing the 6-31G* basis set in Gaussian09. DFT/B3LYP/6-31G* has been found to be an accurate formalism for calculating the structural and optical properties of many molecular systems.

According to this DFT computation, the HOMO and the LUMO energy levels of 4,7-dithienylbenzothiadiazole (DTBT) and DTzBT were −5.29 eV/−2.62 eV and −5.79 eV/−2.93 eV, respectively. As shown in Fig. 1, although both materials had very similar electron density geometries, DTzBT had a lower HOMO and LUMO energy level than did DTBT. This is related to its improved electro-affinity. Since the electro-affinity of DTzBT was increased by introducing thiazole units, that is electron withdrawing molecules, the HOMO and the LUMO energy levels of DTzBT were lower than those of DTBT, although they had similar electron density geometries. Likewise, the HOMO and LUMO energy levels of PCDTBT and PCDTzBT were calculated as −4.99 eV/−2.59 eV and −5.31 eV/−2.87 eV, respectively. As a result of the simulated electronic properties, the synthesized PCDTzBT could have more balanced energy levels than the PCDTBT, which is a well-known polymer used in OPVs.

3.3. Optical properties

Fig. 2(a) shows the UV–vis absorption and photoluminescence (PL) spectrum of PCzTzBT in the chloroform solution and in the thin solid films. PCDTzBT exhibited maximum UV–vis absorption peaks (λ_{max}) at 369/531 nm in solution and 384/562 nm in film. Compared to the solution, PCDTzBT exhibited red-shifted maximum absorption peaks at about 50 nm in film. Maximum emission peak and shoulder peak, in solution, were displayed at 522 nm and 610 nm, respectively. The maximum emission peak at 522 nm comes from the 4,7-dithiazolylbenzothiadiazole unit, and the shoulder peak arises from the molecular orbital overlap between the electron-donating unit and electron-withdrawing unit. Like the UV–vis absorption spectrum, the PL spectrum of the film sample exhibited peaks at longer wavelengths compared to the solution sample. The maximum emission peak and shoulder peak, in solution, were shifted to the long wavelength region. However, in film, the intensity of the DTzBT unit decreased, and the intensity of the emission peak that arose from the molecular orbital overlap greatly increased. This implied that PCDTzBT has a strong inter and intra molecular interaction, from which it seems to have the potential to be a good active material for organic photovoltaics.

Furthermore, the UV–vis absorption range of DTzBT overlapped well with the emission range of polyfluorene, which is the most important blue emitting material, which implies that the DTzBT unit could be introduced as a dopant material for white organic light emitting diodes since efficient energy transfer could proceed from polyfluorene to DTzBT. The UV–vis absorption spectra of DTzBT and the photoluminescence (PL) spectra of polyfluorene are shown in Fig. 2(b).

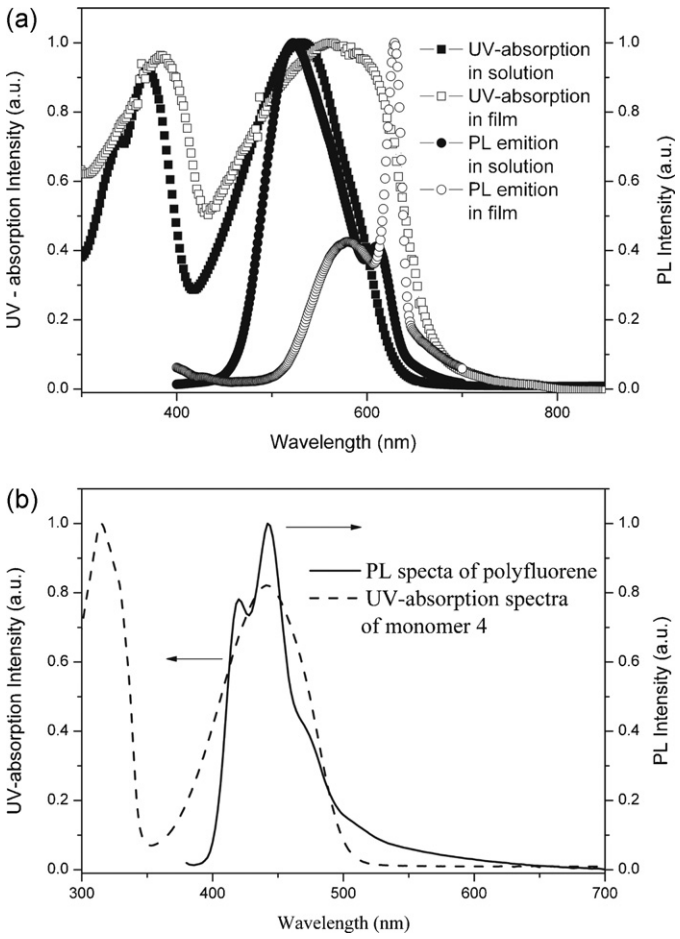

Fig. 2. (a) UV–vis absorption and PL emission spectra of PCDTzBT in a solution (in chloroform at a concentration of 1 mg/mL), and in a film (b) comparison UV–vis absorption spectra of DTzBT with PL emission spectra of polyfluorene.

On the basis of all these optical measurements, it is expected that the DTzBT unit could be used as a potential material unit in OLEDs as well as in OPVs. The optical band gap of PCDTzBT was calculated from the band edge of the UV–vis absorption spectrum in the film. The polymer had a low optical band gap of 1.85 eV.

3.4. Electrochemical properties

The electrochemical behavior of the copolymers was investigated using cyclic voltammetry (CV). The supporting electrolyte was tetrabutyl ammonium hexafluorophosphate (Bu_4NPF_6) in acetonitrile (0.1 M), and the scan rate was 50 mV/s. The ITO glass and Pt plates were used as the working and counter electrodes, respectively, and silver/silver chloride [Ag in 0.1 M KCl] was used as the reference electrode. All of other measurements were calibrated using the ferrocene value of −4.8 eV as the standard. The HOMO levels of the polymers were determined using the oxidation onset value. The LUMO levels were calculated from the differences between the HOMO energy levels and the optical band-gaps, which were determined using the UV–vis absorption onset values in the films.

Fig. 3 shows the cyclic voltammograms of the synthesized polymers. The synthesized polymer, PCDTzBT, showed an electrochemical stability with respect to oxidation and reduction. The oxidation and reduction onset potentials of PCDTzBT were 1.16 V and −0.73 V, respectively. According to these results, the HOMO level of PCDTzBT was −5.54 eV, and the LUMO level was −3.65 eV.

Table 2
Optical, electrochemical data and energy levels of PCDTzBT.

Polymer	Absorption λ_{max} (nm)[a]		PL λ_{max} (nm)[d]		E_g^{op} [e] (eV)	E_{onset}^{ox} [f] (V)	Energy level[g] (eV)	
	Solution[b]	Film[c]	Solution[b]	Film[c]			HOMO	LUMO
PCDTzBT	369, 531	384, 562	522, 610 (sholder)	580 (sholder), 630	1.85	1.16	−5.54	−3.65

[a] λ_{max} was determined from UV–vis data.
[b] Diluted in chloroform.
[c] Spin-coated from a chloroform.
[d] λ_{max} was determined from PL data.
[e] Estimated from the onset of UV–vis absorption data of the thin film.
[f] Onset oxidation potential.
[g] Calculated from the reduction and oxidation potentials under the assumption that the absolute energy level of Fc/Fc^+ was 4.8 eV below a vacuum.

The electrochemical band gap of PCDTzBT from the electrochemical measurement was 1.89 eV, which almost coincided with the optical band gap. The electrochemical properties of the polymers are summarized in Table 2.

3.5. Photovoltaic properties

PCDTzBT molecules were applied in a bulk heterojunction geometry (BHG) with PCBM. The OPV cells were fabricated with a sandwiched glass/ITO/PEDOT:PSS/polymer-PCBM (1:4, w:w)/BaF_2/Ba/Al structure. After all of the fabricated devices were encapsulated in a glove box, the I–V characteristics were measured under an ambient atmosphere (Table 3).

Fig. 4 illustrates the I–V properties of the fabricated devices. Since $PC_{71}BM$ has a stronger UV–vis absorption property than does $PC_{61}BM$ in the visible region, especially around 500 nm [24], $PC_{71}BM$ was used as the acceptor material. As shown in Fig. 4, PCDTzBT exhibited the best performance (0.535 V of V_{OC}, 2.8 mA/cm^2 of J_{SC}, 0.3 of FF, and 0.448% of power conversion efficiency (PCE)) in the device where 80 wt% $PC_{71}BM$ was contained in the active layer (pol:PCBM = 1:4, w/w). Nevertheless, a PCE of 0.448% was relatively low value. It was likely to originate from low molecular weight that was dependent upon rigid backbone structure of PCDTzBT. The PCE values of devices were increased with increase of weight ratio of $PC_{71}BM$, which stemmed from photo electron generation property of $PC_{71}BM$. It could be confirmed from differences of J_{SC} values and EQE data (Fig. 5).

In order to optimize photovoltaic property of organic photovoltaic devices based on PCDTzBT, $PC_{61}BM$ and $PC_{71}BM$ were introduced as acceptor materials in order to confirm the acceptor effect in the polymer/acceptor material blend. PCDTzBT exhibited V_{OC} values of 0.515 V and J_{SC} values of 1.8 mA/cm^2 when $PC_{61}BM$ was used as the acceptor. On the other hand, when $PC_{71}BM$ was used, the V_{OC} values (0.535 V) were similar to the V_{OC} values that were measured when $PC_{61}BM$ was used as the acceptor. However, the J_{SC} values increased to 2.8 mA/cm^2. In spite of low HOMO energy level of PCDTzBT, all of the devices, where PCDTzBT was introduced as an active materials, appeared low V_{OC} values. It originated from poor solubility of PCDTzBT, which was followed by rigid backbone structure. V_{OC} value was affected by morphology characteristics as well as the HOMO energy level of donor materials. Poor solubility of PCDTzBT had a bad effect on forming an active layer film, which was supposed to be a reason of low V_{OC} values.

As shown in Table 4, PCE values were increased with decrease of active layer thickness. In general, in the case of a polymer that had

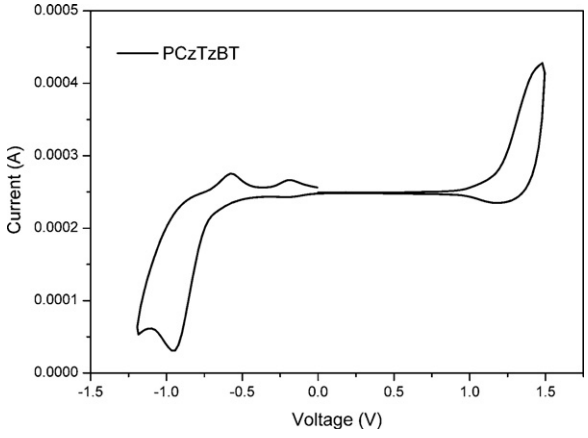

Fig. 3. Cyclic voltammograms of thin films recorded in 0.1 M Bu_4NPF_6/acetonitrile at a scan rate of 50 mV/s.

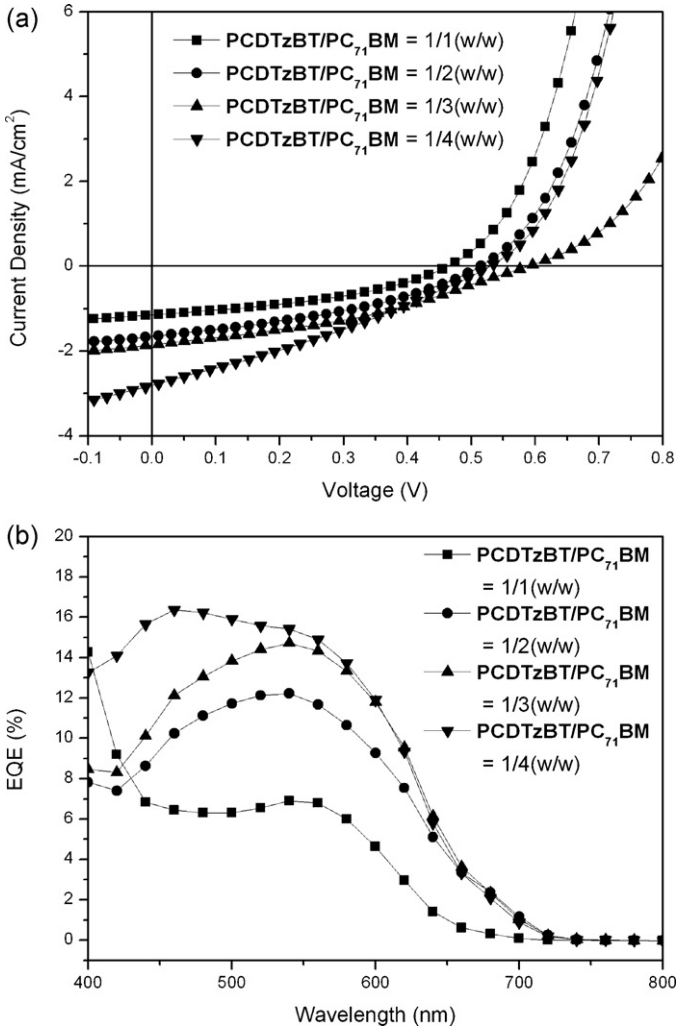

Fig. 4. Comparison of (a) I–V characteristics and (b) EQE properties of photovoltaic devices with different weight ratio of $PC_{71}BM$ in active layers.

Table 3
Potovoltaic property of devices with different weight ratio of PC71BM in active layers.

Active layer	Spin coating speed (rpm)	J_{SC} (mA/cm^2)	V_{OC} (V)	FF	η (%)
PCDTzBT/PC_{71}BM = 1/1 (w/w)	1400	1.1	0.455	0.41	0.211
PCDTzBT/PC_{71}BM = 1/2 (w/w)	1400	1.6	0.515	0.38	0.318
PCDTzBT/PC_{71}BM = 1/3 (w/w)	1400	1.8	0.596	0.36	0.392
PCDTzBT/PC_{71}BM = 1/4 (w/w)	1400	2.8	0.535	0.30	0.448

Photovoltaic properties of all of the devices were measuered under AM 1.5 simulated solar illumination at an irradiation intensity of 100 mW cm^{-2}.

Table 4
Photovoltaic property of devices that have PCDTzBT/PCBM (1:4, w/w) blend films as active layers.

Active layer[a]	Spin coating speed (rpm)	Thickness (nm)	J_{SC} (mA/cm^2)	V_{OC} (V)	FF	η (%)
PCDTzBT/PC_{61}BM	500	120	1.5	0.515	0.33	0.251
PCDTzBT/PC_{61}BM	800	70	1.8	0.495	0.33	0.291
PCDTzBT/PC_{61}BM	1100	60	1.8	0.515	0.33	0.310
PCDTzBT/PC_{61}BM	1400	40	1.8	0.495	0.34	0.309
PCDTzBT/PC_{71}BM	500	120	2.0	0.535	0.31	0.324
PCDTzBT/PC_{71}BM	800	70	2.6	0.535	0.30	0.411
PCDTzBT/PC_{71}BM	1100	60	2.7	0.535	0.30	0.435
PCDTzBT/PC_{71}BM	1400	40	2.8	0.535	0.30	0.448

Photovoltaic properties of all of the devices were measuered under AM 1.5 simulated solar illumination at an irradiation intensity of 100 mW cm^{-2}.
[a] Polymer:PCBM = 1:4 (w/w).

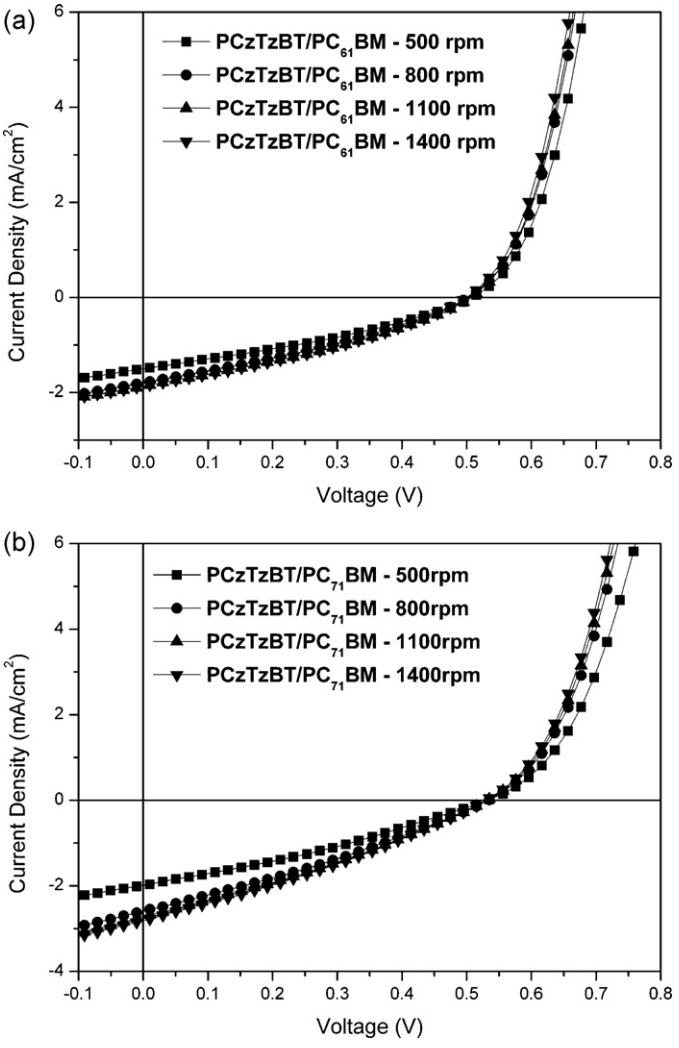

Fig. 5. I–V characteristics of photovoltaic devices (polymer:PCBM = 1:4) that have (a) PCDTzBT/PC_{61}BM, and (b) PCDTzBT/PC_{71}BM blend films as active layers.

good charge transport property, PCE values were increased with increase of active layer thickness. However, as mentioned above, it was expected that PCDTzBT had poor charge transport property due to low molecular weight and poor film forming property, which had an effect on relationships between the thickness and performances of PV cells. As expected, the best performance data were obtained in the device that used the PCDTzBT/PC_{71}BM blend film as the active layer, which corresponded to a V_{OC} of 0.535 V, a J_{SC} of 2.8 mA/cm^2, a FF of 0.3, and a PCE of 0.448%. It is likely that the asymmetric PC_{71}BM had an increased absorption in the visible region, which leads to better overlap with the solar spectrum relative to that obtained with the PC_{61}BM. Nevertheless, low PCE values were obtained in devices that included PCDTzBT in their active layers, which resulted from its low molecular weight. Since a short conjugation length was present in the conjugated main chain and this allowed PCDTzBT to have a poor molecular orbital overlap effect, which resulted from its low molecular weight, between the electron-donating unit and electron-withdrawing moiety, photoelectron generation and transport were restricted. In spite of the low molecular weight, since PCDTzBT exhibited well-balanced energy levels and strong intermolecular interactions, it is seems that PCDTzBT is worth further study. The photovoltaic properties of PCDTzBT are summarized in Table 4.

4. Conclusions

In summary, PCDTzBT that was based on carbazole and DTzBT was successfully synthesized through the Suzuki coupling reaction for used in OPVs. These copolymers exhibited low band gaps of 1.85 eV and well balanced HOMO and LUMO energy levels of −5.54 and −3.65 eV, respectively. Although the low molecular weight prohibited PCDTzBT to have as high a PCE value as PCDTBT, it is expected that PCDTzBT will improve the photovoltaic properties of devices by optimizing polymerization conditions and with the introduction of alkyl chains. Moreover, various polymers involving the DTzBT moiety could be used in OLEDs due to its optical property.

Acknowledgements

This research was supported by a grant from the Fundamental R&D Program for Core Technology of Materials funded by the Ministry of Knowledge Economy, Republic of Korea.

This work was supported by the New and Renewable Energy R&D program (2008-N-PV08-02) under the Korea Ministry of Knowledge Economy (MKE).

References

[1] E. Perzon, X. Wang, F. Zhang, W. Mammo, J.L. Delgado, P. de la Cruz, O. Inganäs, F. Langa, M.R. Andersson, Synth. Met. 154 (2005) 53–56.
[2] C. Shi, Y. Yao, Y. Yang, Q. Pei, J. Am. Chem. Soc. 128 (2006) 8980–8986.
[3] M. Jørgensen, K. Norrman, F.C. Krebs, Sol. Energy Mater. Sol. Cells 92 (2008) 686–714.
[4] Y. Li, Y. Zou, Adv. Mater. 20 (2008) 2952–2958.
[5] Y.J. Cheng, S.H. Yang, C.S. Hsu, Chem. Rev. 109 (2009) 5868–5923.
[6] H. Xin, X. Guo, F.S. Kim, G. Ren, M.D. Watson, S.A. Jenekhe, J. Mater. Chem. 19 (2009) 5303–5310.
[7] M. Skompska, Synth. Met. 160 (2010) 1–15.
[8] M. Helgesen, R. Søndergaard, F.C. Krebs, J. Mater. Chem. 20 (2010) 36–60.
[9] T.Y. Chu, J. Lu, Y. Zhang, J.R. Pouliot, S. Wakim, J. Zhou, M. Leclerk, Z. Li, J. Ding, Y. Tao, J. Am. Chem. Soc. 113 (2011) 4250–4253.
[10] M. Zhang, H.N. Tsao, W. Pisula, C.Y.A.K. Mishra, K. Müllen, J. Am. Chem. Soc. 129 (2007) 3472–3473.
[11] S. Allard, M. Forster, B. Souharce, H. Thiem, U. Scherf, Angew. Chem. Int. Ed. 47 (2008) 4070–4098.
[12] B.S. Ong, Y. Wu, Y. Li, P. Liu, H. Pan, Chem. Eur. J. 14 (2008) 4766–4778.
[13] B.L. Lee, K.M. Han, E.K. Lee, I.N. Kang, D.H. Kim, S. Lee, Synth. Met. 159 (2009) 132–136.
[14] J. Liu, X. Guo, L. Bu, Z. Xie, Y. Cheng, Y. Geng, L. Wang, X. Jing, F. Wang, Adv. Funct. Mater. 17 (2007) 1917–1925.
[15] J.Y. Lee, M.H. Choi, D.K. Moon, J.R. Haw, J. Ind. Eng. Chem. 16 (2010) 395–400.
[16] M.J. Park, J.I. Lee, H.Y. Chu, S.H. Kim, T. Zyung, J.H. Eom, H.K. Shim, D.H. Hwang, Synth. Met. 159 (2009) 1393–1397.
[17] K.W. Song, J.Y. Lee, S.W. Heo, D.K. Moon, J. Nanosci. Nanotechnol. 10 (2010) 99–105.
[18] K.S. Yook, J.Y. Lee, J. Ind. Eng. Chem. 16 (2010) 181–184.
[19] J. Hou, H-Y. Chen, S. Zhang, G. Li, Y. Yang, J. Am. Chem. Soc. 130 (2008) 16144–16145.
[20] J.Y. Lee, W.S. Shin, J.R. Haw, D.K. Moon, J. Mater. Chem. 19 (2009) 4938–4945.
[21] J.Y. Lee, S.W. Heo, H. Choi, Y.J. Kwon, J.R. Haw, D.K. Moon, Sol. Energy Mater. Sol. Cells 93 (2009) 1932–1938.
[22] H.Y. Chen, J. Hou, S. Zhang, Y. Liang, G. Yang, Y. Yang, L. Yu, Y. Wu, G. Li, Nat. Photon. 3 (2009) 649–653.
[23] L. Huo, J. Hou, S. Zhang, H-Y. Chen, Y. Yang, Angew. Chem. Int. Ed. 49 (2010) 1500–1503.
[24] J. Peet, J.Y. Kim, N.E. Coates, W.L. Ma, D. Moses, A.J. Heeger, G.C. Bazan, Nat. Mater. 6 (2007) 497–500.
[25] E. Bundgaard, F.C. Krebs, Sol. Energy Mater. Sol. Cells 91 (2007) 954–985.
[26] N. Blouin, A. Michaud, D. Gendron, S. Wakim, E. Blair, R. Neagu-Plesu, M. Belletête, G. Durocher, Y. Tao, M. Leclerc, J. Am. Chem. Soc. 130 (2008) 732–742.
[27] M.T. Bernius, M. Inbasekaran, J. O'Brien, W. Wu, Adv. Mater. 12 (2000) 1737–1750.
[28] J. Liu, Z. Xie, Y. Cheng, Y. Geng, L. Wang, X. Jing, F. Wang, Adv. Mater. 19 (2007) 531–535.
[29] J. Luo, X. Li, Q. Hou, J. Peng, W. Yang, Y. Cao, Adv. Mater. 19 (2007) 1113–1117.
[30] J. Liu, Y. Cheng, Z. Xie, Y. Geng, L. Wang, X. Jing, F. Wang, Adv. Mater. 20 (2008) 1357–1362.
[31] M. Akhtaruzzaman, N. Kamata, J. Nishida, S. Ando, H. Tada, M. Tomura, Y. Yamashita, Chem. Commun. 318 (2005) 3–3185.
[32] G. Chen, S. Lan, P. Lin, C. Chu, K. Wei, J. Polym. Sci. A: Polym. Chem. 48 (2010) 4456–4464.
[33] N. Kobayashi, R. Koguchi, M. Kijima, Macromolecules 39 (2006) 9102–9111.
[34] X. Li, W. Zeng, Y. Zhang, Q. Hou, W. Yang, Y. Cao, Eur. Polym. J. 41 (2005) 2923–2933.
[35] R. Yang, R. Tian, J. Yan, Y. Zhang, J. Yang, Q. Hou, W. Yang, C. Zhang, Y. Cao, Macromolecules 38 (2005) 244–253.
[36] N. Blouin, A. Michaud, M. Leclerc, Adv. Mater. 19 (2007) 2295–2300.